

NEGATIVE PION BEAMS FOR RADIOTHERAPY *

M. R. Raju

Los Alamos Scientific Laboratory
Los Alamos, New Mexico

1. Introduction

Significant progress has been made in radiation therapy over the past two decades. This progress is mainly due to better understanding of the biology of cancer, better dosimetry, and use of high energy radiations in therapy.

Ideally, one would like to deliver a tumoricidal dose to the tumor, but in practice the dose that can be given to the tumor is limited by the injury to normal tissues both within and outside the treatment volume. Normal tissue injury depends on the volume irradiated; the smaller the volume, the greater the dose the normal tissue can likely withstand. It is possible to deliver tumoricidal doses to the tumor without undue normal tissue reactions if the high dose region can be restricted to the tumor volume and if the dose to normal tissue is kept to a minimum. How well this can be done depends on the location of the tumor, the physical properties of the radiation, and the techniques used.

The critical margin between the tumor control and the production of complications is illustrated in Figure 1, You can see from the figure that complications restrict the dose to be given to tumor volume to increase percent tumor control. If we could displace the tumor control curve to lower doses and/or decrease the damage to normal tissues within and outside the treatment volume, thereby displacing the complications curve to higher doses, one could expect further improvements in radiation therapy (Boone and Wiley, 1971). Today we are discussing the potential applications of protons, heavy ions and π^- mesons with the hope that these new radiations could make further significant improvements in radiation therapy.

As I mentioned before that significant progress in radiation therapy has been made over the past two decades. In spite of these developments, unfortunately, failure is still common. Suit (1969) estimated that, of 175,000 cancer deaths per year in the United States occurring despite treatment with radiotherapy, nearly 58,000 can be attributed to local or regional failure. The failure to cure is generally due to inability to give tumoricidal doses without undue reaction to normal tissue as illustrated in Figure 1.

* Work performed under auspices of the U. S. Atomic Energy Commission.

The object of radiation therapy is to sterilize all cancer cells in the treatment volume and yet make it possible for the normal vital structures within the treatment volume to survive and eventually repopulate the treatment volume. Now, you might wonder, in spite of the availability of high-energy radiations with the better dose localization characteristics, what is preventing us to do this? Many tumors have inadequate blood supply, and hence they may contain a small proportion of hypoxic cells.* For conventional radiation, the dose required to sterilize hypoxic cells is about three times that compared to oxygenated cells. The presence of hypoxic cells in the tumor therefore requires an increase in the tumoricidal dose. It is known however, that in certain types of animal tumors - - and therefore probably in human tumors as well - - an increasing proportion of hypoxic cells of the tumor become oxygenated during fractionated radiotherapy. (See Van Putten and Kallman, 1968.) Thus, the hypoxic cells that are oxygenated during the treatment are not so resistant to subsequent fractions of radiotherapy. It may therefore be possible to overcome the oxygen effect by fractionation with conventional radiation alone for some less advanced stages of cancer. However, reoxygenation may not take place for advanced tumors. As Dr. Todd has pointed out, the radiation resistance of hypoxic cells when compared to oxygenated cells is reduced with increasing LET. Thus, high LET radiations may be more effective in overcoming the hypoxic cell problem where the current methods are not successful. However, it must be pointed out that hypoxic cells as a limiting factor in radiation therapy is proven radiobiologically but not clinically so far. (Kaplan, 1970.)

It is also known, as Dr. Todd has pointed out, that the radiation sensitivity of cells for conventional radiations depends upon their stage in their cell cycle. It could be that in situations where we are not able to treat successfully with conventional radiations, it is possible that the resistant cells are increasing as the treatment proceeds, thereby making it difficult to sterilize all the cells in the tumor. Clinical experience with conventional radiations shows large differences in radiation responses of human tumors. For high LET radiations however, the radiation sensitivity variations as a function of cell cycle and the presence or absence of oxygen are relatively less important. (Sinclair 1969, Bird 1971.) Hence, high

*Cells lacking supply of oxygen.

LET radiations may provide a more uniform response of different tumors. It may be possible to exploit further the differences between normal and malignant tissues by using high LET radiations in the treatment of resistant tumors.

The rationale of using radiations such as protons, heavy ions, and π^- mesons is twofold: first of all, the improved depth dose distributions (as Dr. Todd pointed out - - the dose deposited by these radiations increases with depth, whereas for conventional radiations the dose decreases - - with depth except for the initial buildup); and in addition, depending upon the particles that you use, we could also overcome other problems such as hypoxic cells, stage sensitivity variations, and variations of radiation sensitivity from tumor to tumor as mentioned above. The combination of excellent dose localization characteristics of these heavy charged particles and relatively high LET in the treatment volume may be of potential value in radiation therapy. With this background let me then confine my remarks only to π^- mesons.

The potential application of negative pions in radiotherapy has been appreciated by many people. Fowler and Perkins (1961) were the first to make detailed calculations, and this work generated heightened interest in the use of π^- mesons for therapy.

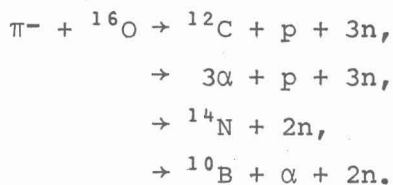
2.1 Interactions of Pi Mesons with Matter

The pi mesons (also called pions) are positive, negative, or neutral, and are secondary particles produced in a nuclear interaction. They are all unstable. Neutral pions have a very short lifetime, 10^{-16} seconds, and usually decay into two gamma rays. Charged pions are relatively more stable than neutral pions. They have a mean lifetime of 2.54×10^{-8} seconds, hence some of them decay in flight to muons and then electrons. Negative pions are the particles of interest in radiotherapy.

A π^- meson has a mass 273 times that of an electron, or approximately 15% of the mass of a proton. Thus, it shares the properties of heavy charged particles. The mass being lower when compared to protons, pions scatter three times as much as protons. π^- mesons will have the usual Bragg curve, and in addition, the unique property of getting captured by a nucleus of the medium when it comes to rest. When the π^- is captured by hydrogen, the

resulting hydrogen atoms will have π^- in the electronic orbit in place of the electron. The hydrogen atom diffuses through the medium. When this atom gets close to a heavier nucleus, the pion is often transferred to the heavier atom because the resulting binding energy is lower. As a result, the pion is captured by the main tissue elements and cascades down the atomic levels in a time that is short compared with its lifetime. During the cascade, characteristic X rays are emitted; they are called pi mesic X rays. This is illustrated in Figure 2. These X rays are of special interest and are discussed below. The π^- , when in the lower atomic orbit, spends a considerable fraction of the time inside the nucleus, because (its mass being 273 times that of an electron) the pion orbits are only 1×273 as large as electron orbits. The pion is absorbed by the nucleus, and the π^- rest mass of 140 MeV appears in the form of kinetic energy of nuclear fragments, except for about 40 MeV, which is used in overcoming the binding energy of the nucleus. Nearly 70 MeV appears in the form of kinetic energy of neutrons, and the rest (about 30 MeV) in the form of the kinetic energy of the charged particles, such as protons, alpha particles, and heavier particles that are absorbed locally (Fowler and Perkins, 1961). Thus, for π^- , the capture process enhances the dose near the Bragg peak region due to these short-range and heavily-ionizing fragments. It is this unique characteristic of the π^- that makes it promising in radiotherapy. Examples of π^- capture as observed in a nuclear emulsion are shown in Figure 3. The disruption of the nucleus is often referred to as "star formation", because, when it was first observed in a nuclear emulsion, the tracks looked like a star.

In bone-free parts of the body, about 73% of π^- mesons are captured in oxygen, 20% in carbon, 3% in nitrogen, and 4% in heavier atoms. (Fowler and Mayes, 1967) Fowler and Mayes found that interactions with oxygen produced various tracks due to particles of different charges. Some of the dominant reactions in oxygen are:



The type of the particle, its energy, and frequency per capture in water, as measured by Fowler and Mayes (1967) are shown in Table I.

Table I
Energy Partition for π^- Capture in Water

| <u>Particle type</u> | <u>Average energy per pion star (MeV)</u> | <u>Average number of particles per pion star</u> |
|-----------------------------|-------------------------------------------|--------------------------------------------------|
| Protons | 15.2 | 0.95 |
| Deuterons | - - | - - |
| α Particles | 7.8 | 0.99 |
| Heavy recoils $Z \geq 3$ | 4.4 | 0.78 |
| Neutrons | 69.0 | 2.7 |

The capture reactions in carbon, nitrogen, and oxygen are quite similar in their yield of protons and alpha particles and their mean energies. The energy spectrum of each type of particle covers a wide range.

The phenomenon of pion capture, on the average, yields one singly-charged particle (protons, deuterons, or tritons), one alpha particle, one heavy particle ($Z \geq 3$), and three neutrons. The dose contributed locally by the neutrons is small compared with the other components in the star. Although protons contribute considerable dose, it is the alpha particles that produce considerable biological effect. Heavy recoils also produce significant biological effect, since their ranges extend up to 20 microns in tissue, with an average of about 8 microns.

About 2% of stopping pions produce high-energy gamma rays, peaking in the energy region of about 100 MeV (Davies et al., 1966). These gamma rays are of special interest and are discussed below.

2.2 Production of Pions with Protons

I will give you a brief description of pion production at the 184-in. cyclotron at Berkeley to give you a better idea about a pion beam and its composition. The setup is shown in Figure 4. The accelerated protons from this accelerator strike a beryllium target and produce π^- , π^+ and π^0 . The

π^- mesons are deflected out of the cyclotron through a vacuum window by the cyclotron fringe field, which works as the first bending magnet.* The beam is then focused by a quadrupole focusing magnet (meson quad) and passes along a channel through the main cyclotron shielding (dotted area). The energy of the beam is selected by adjusting the current in the bending magnet, and the beam is focused again by another quadrupole focusing magnet.

2.3 Pion Beam Contamination

Neutral pions produced in the target decay into two gamma rays because of their short lifetime of 10^{-16} sec. The gamma rays are converted into electron-positron pairs in the target. The electrons from this conversion constitute the electron background in the π^- beam. Charged pions have a mean life of 2.54×10^{-8} sec, hence some of them decay in flight; this contributes the muon background. The muons and electrons that have the same momentum as the pions selected by the bending magnet remain in the beam. The range of muons is about 30% greater than pions of the same momentum, and the electrons have a much higher range. For a beam of momentum 140 MeV/c, the range of π^- is ~ 12 cm of water, $\mu^- \sim 16$ cm, and $e^- \gg 30$ cm. The muon and electron contamination in a pion beam can be reduced by using radio-frequency or electrostatic separators. These separators select particles by velocity selection.

2.4 Range Energy

The range of π^- in water, as a function of energy, is shown in Figure 5. In radiation therapy, pions with energy of about 40 to 70 MeV are of interest. The momentum of a particle is often used in high energy physics in addition to energy. The energy selection of particle beams is done by magnetic fields. The bending of a particle in a given magnetic field is proportional to its momentum. The plot of energy versus momentum for pions is shown in Figure 6.

2.5 Pion Decay

I want to remind you again here that pions are not stable particles.

*The charged-particle beams are made by using focusing and bending magnets. The principles of beam optics are similar to geometric optics. The beam is focused by quadrupole magnets, and their focusing properties are similar to a lens in geometric optics. The energy selection of the beam is made by using bending magnets and their properties are similar to prisms in geometric optics.

They have a very short half life. Low-energy pions decay much faster than high energy pions. A distance of about 5 to 10 meters between the target and the experimental area is generally required to allow the necessary shielding against the intense flux of neutrons and gamma rays produced in the target and to accommodate the magnetic system needed to deliver pions of the desired energy to the experimental area. Figure 7 shows the percentage of original π^- remaining in the beam after it has traveled about 5 and 10 meters. Thus, it can be seen from the figure that nearly 75 and 50% of pions in the energy range of interest to radiotherapy decay in flight in drifting to a distance of 10 and 5 meters, respectively. The resulting muons have a broad energy spectrum. Muons having the same momentum as pions selected by the magnetic system remain in the beam as contamination. Because of this decay it is not practical to use energies much lower than about 40 MeV. Even for a short beam path of about 5 meters, nearly 50% of the mesons decay, and hence, if we want to consider using π^- mesons in therapy, it is very important to have as intense a beam as possible.

2.6 Depth-Dose and LET Distribution of π^- Mesons

The pion depth-dose distributions as calculated by Curtis (Curtis and Raju, 1968) for a beam of energy 95 MeV with a contamination of 10% μ^- and 25% e^- , and for a beam with no contamination, are shown in Figures 8 and 9 respectively. Electron and muon contaminations in the beam reduce the peak-to-plateau ratio and contribute dose beyond the treatment volume. The LET distribution of π^- at the peak of depth-dose distribution in water is shown in Figure 10. The contributions from the various components of the beam are shown in the figure. The area under the curve is proportional to the dose. It can be seen from the figure that even at the peak of depth-dose distribution, a substantial part of the total dose is due to pions that are still slowing down. Most of the protons from star formation are of low LET. The alpha particles and heavy recoils are of high LET, and the LET of heavy recoils extends up to 900 KeV/ μ . For a pure pion beam the percent dose contribution at the peak, of the depth-dose distribution due to pions passing the peak, is 35%; that due to protons from stars is 33%; that due to heavily ionizing components, such as alpha particles and heavy recoils, is 25%; and that due to neutrons is about 7%. Thus, at the peak region, the component due to LET values greater than 30 KeV/ μ is about 30%, and this fraction varies

significantly over the peak region. This high LET decreases with increasing width of the Bragg peak.

Physical measurements have been carried out at the 184-in synchrocyclotron at Berkeley (Raju, et al., 1971a) and at the CERN synchrocyclotron at Geneva (Sullivan and Baarli, 1968). Some measurements were also made at the Brookhaven cosmotron (Tisljar-Lentulis, et al., 1971). The depth dose distribution of π^- mesons measured at Berkeley is shown in Figure 11. The increase in dose for π^- beam over π^+ is due to the star events. The experimental measurements, in general, are in agreement with theoretical expectations (Turner, et al., 1970).

As discussed before, pi mesic X rays and γ rays are also emitted from the region where the π^- stop and produce stars. The dose contribution due to X rays and γ rays is small. However, significant numbers of these radiations may be detected outside the exposed patient, and this may provide a good method of externally observing the stopping pion region for planning treatment and for monitoring during exposure. Experimental results indicate this can indeed be done in principle (Sperinde et al., 1971; Dean and Holm, 1971). Another interesting possibility of locating the stopping pion region is to look at the positron activity induced by the stopping pions after irradiation (Taylor et al., 1970). Such measurements would be helpful to keep the record of treatment volume.

3. Pion Radiobiology

The current sources of negative pi mesons do not have adequate intensity to do the necessary radiobiology and therapy with them. The Berkeley 184-in. synchrocyclotron is the most intense source of low-energy pions currently available. Even there the dose rates available are in the range of 5 - 60 rad/hr at the peak, depending on the size of the beam. This intensity, however, is not adequate for the necessary pretherapeutic radiobiological work. Some measurements of RBE and OER have been made by using different biological systems that are sensitive enough for the intensity of the pion beam available. Most of these measurements have been made at only two points in the depth-dose distribution, one at the beam entrance and the other at the peak of the depth-dose distribution. The contaminated beam was used in all the radiobiological work since purification of the beam reduces the pion intensity considerably.

The beam has a contamination of 25% electrons and 10% muons. At the beam entrance these contaminants deposit nearly 30% of the dose. At the peak the beam contamination deposits nearly 10 - 15% of the dose. Most of the radiobiological work has been published in the literature and some of the work is being published now. A summary of these results is given in Table II and Table III. As an example, I will just present briefly RBE and OER measurements at the pion peak using bean roots and human kidney cells in culture.

The OER was relatively independent of dose rate when the bean roots were exposed at low temperatures (Hall and Cavanagh, 1967). The OER for π^- mesons at the peak was measured when the roots were exposed at low temperature (4°C). The results of a 10-day growth, plotted as a function of dose, are shown in Figure 12. (Raju et al., 1970.) The OER was found to be 1.5.

Human kidney cell survival curves for π^- mesons at the peak in the presence of air or nitrogen are shown in Figure 13. Also shown in the figure is the survival curve for ^{60}Co gamma rays at a dose rate such that the cell exposure was of the same duration as for mesons. The dose rate of pions is about 25 rads/hr, and the dose rate of ^{60}Co is about 1 rad/min. The RBE and OER for π^- mesons calculated at 10% level are 2.5 and 1.6 respectively. (Raju et al., 1971b.)

The biological results could be summarized as follows. Depending on the biological end point and the system used, the RBE value at the peak is in the region of 2 to 5 and the RBE at the plateau is 1.

Table II. RBE of π^- mesons at the peak of depth-dose distribution^a

| <u>Biological system</u> | <u>RBE</u> | <u>Reference</u> |
|--------------------------------------------------------|------------|---------------------------|
| Abnormal anaphases in <u>Vicia faba</u> root meristems | 2.4 | Richman et al. (1967) |
| <u>Vicia faba</u> , 10-day growth | 3 | Raju et al. (1970) |
| Arginine reversions in yeast | 1.8 | Raju et al. (1971c) |
| Proliferative capacity of ascites tumor cells | 5 | Feola et al. (1968, 1970) |
| Polyploidy induction in ascites tumor cells | 2.5 | Loughman et al. (1968) |
| Human kidney cells T-1 | 2.5 | Raju et al. (1971b) |
| Human kidney cells in frozen state | ~ 2 | Burki et al. (1969) |
| Human lymphocytes | 2 | Madhvanath (1971) |
| Spermatogonia | 3.7 | Baarli et al. (1971) |

^aRBE of π^- mesons at the plateau is 1.

Table III. OER of π^- mesons at the peak of depth-dose distribution^a

| <u>Biological system</u> | <u>OER</u> | <u>Reference</u> |
|------------------------------|------------|---------------------|
| <u>Vicia faba</u> (growth) | 1.35- 1.5 | Raju et al. (1970) |
| Arginine reversions in yeast | 1.5 - 1.8 | Raju et al. (1971c) |
| Human kidney cells T-1 | 1.6 | Raju et al. (1971b) |

^aOER at the plateau is expected to be the same as for conventional radiation, i.e., 2.6.

The OER values at the peak of the depth dose distribution are in the region of 1.5 to 1.8. For a pure pion beam, the RBE values at the peak will be slightly higher and the OER slightly lower. However, these values change according to the width of the peak. With increasing width, the RBE decreases and the OER increases. The RBE and OER at the beam entrance are expected to be the same as for conventional radiations.

I have recently completed a chapter on physical and biological aspects of negative pions in radiotherapy and it will be published soon in Current Topics in Radiation Research. The potential uses of π^- mesons in radiotherapy

was discussed by Kaplan (1969), Elkind (1970), Bond (1971), Todd (1971), and Whitmore (1971).

The physical and radiobiological measurements of π^- mesons indicate the following: The intervening normal tissue receives low dose at an LET similar to that of conventional radiation. The treatment volume receives higher dose at high LET which increases the biological effect there and, in addition, increases the damage to hypoxic cells. Intervening normal tissues recover more than the cells in the treatment volume. Fractionation enhances the damage to the treatment volume when compared to the intervening normal tissues. Thus, π^- mesons offer the additional advantage of favorable biological factors due to differences in the quality of radiation.

Pion facilities with intensities adequate for therapy are being built at Los Alamos, New Mexico, Vancouver, B.C., and Zurich, Switzerland. (Rosen, 1966, 1971). Figure 14 shows the Los Alamos Meson Facility construction progress. Therapeutic facilities are being built at all the three accelerators. Also, a pion facility using the Stanford superconducting electron linear accelerator is being built at Stanford, California. All these facilities are expected to be in operation by 1973 - 1974.

Simultaneous developments of precise tumor-localization techniques are essential to take advantage of sharp dose localization properties of heavy charged particles.

REFERENCES

- BAARLI, J., BIANCHI, M., SULLIVAN, A. H. and QUINTALIANI, M. 1971. Int. J. Radiat. Biol. 19 537.
- BIRD, D. 1971. Sensitivity of synchronized mammalian cells to high-LET radiation, Ph.D. Thesis. (Donner Laboratory, Lawrence Radiation Laboratory report, to be issued.)
- BOND, V. P. 1971. Negative pions: Their possible use in radiotherapy. Am. J. Roentgenol. Rad. Therapy and Nuclear Medicine. 111 9.
- BOONE, M. L. M., WILEY, A. L., Jr. 1971. IEEE Trans. Nucl. Sci. NS-18 3 36.
- BURKI, H. J., BARENDSEN, G. W., RAJU, M. R., AMER, N. M., and CURTIS, S. B. 1969. A method to determine the acute radiation response of human cells to π^- mesons. In: Biology and Medicine Semiannual Report, Lawrence Radiation Laboratory report UCRL-18793, p. 100.
- CURTIS, S. B. and RAJU, M. R. 1968. Radiation Res. 34 239.
- DAVIES, H., MUIRHEAD, H. and WOULD'S, J. N. 1966. Nucl. Phys. 78 673.
- DEAN, P. N. and HOLM, D. M. 1971. Pion stopping region visualization experiments. Radiation Res. 48 201.
- ELKIND, M. M. 1970. Radiobiological considerations in the applications of π^- mesons to radiotherapy. Los Alamos Scientific Laboratory report LA-4602-MS.
- FEOLA, J. M., RICHMAN, C., RAJU, M. R., CURTIS, S. B. and LAWRENCE, J. H. 1968. Radiation Res. 34 70.
- FEOLA, J. M., RAJU, M. R., RICHMAN, C. and LAWRENCE, J. H. 1960. Radiation Res. 44 637.
- FOWLER, P. H. and PERKINS, D. H. 1961. Nature 189 524.
- FOWLER, P. H. and MAYES, V. M. 1967. Proc. Phys. Soc. (London) 92 377.
- HALL, E. J. and CAVANAGH, J. 1967. Brit. J. Radiol. 40 128.
- KAPLAN, H. S. 1969. Potentialities of negative π^- meson beams in radiotherapy of cancer. In: Proceedings of the Third LAMPF Users Meeting, Oct. 29, Los Alamos Scientific Laboratory report LA-4397-MS, p.31.
- KAPLAN, H. S. 1970. Radiation Res. 43 460.
- LOUGHMAN, W. D., FEOLA, J. M., RAJU, M. R. and WINCHELL, H. S. 1968. Radiation Res. 34 56.
- MADHVANATH, U. 1971. Effects of densely ionizing radiations on human lymphocytes cultured in vitro. Ph.D. Thesis. University of California Radiation Laboratory Report UCRL 20680.

- RAJU, M. R., AMER, N. M., GNANAPURANI, M. and RICHMAN, C. 1970. Radiation Res. 41 135.
- RAJU, M. R., LAMPO, E., CURTIS, S. B., and RICHMAN, C., 1971a. Dosimetry of π^- mesons using scintillation detectors and plastic scintillators. Phys. Med. Biol., Vol 16 599-610.
- RAJU, M. R., GNANAPURANI, M., MARTINS, B. I., RICHMAN, C., and BARENDSSEN, G. W., 1971b. RBE and OER of π^- mesons for damage to cultured T-1 cells of human kidney origin, University of California Radiation Laboratory Report UCRL-20669, to be published in Brit. J. Radiol.
- RAJU, M. R., GNANAPURANI, M., STACKLER, B., MARTINS, B. I., MADHVANATH, U., HOWARD, J., LYMAN, J. T., and MORTIMER, R. K. 1971c. Radiation Res., 47, 635-643 (1971).
- RICHMAN, S. P., RICHMAN, C., RAJU, M. R., and SCHWARTZ, B. 1967. Radiation Res. Suppl. 7 182.
- ROSEN, L. (Dec. 1966), Phy. Today, Vol. 19 (No. 12).
- ROSEN, L. (1971), The Los Alamos Meson Physics Facility, A New Tool for Basic Research and Practical Applications, Los Alamos Scientific Laboratory preprint No. LA-DC-12140.
- SINCLAIR, W. K. 1969. Dependence of radiosensitivity upon cell age. In: Proceedings of Time and Dose Relationships in Radiation Biology as Applied to Radiotherapy, Carmel, California, Sept. 15-18, 1969. Brookhaven National Laboratory Report BNL-50203 (C-57) p. 97.
- SPERINDE, J., PEREZ-MENDEZ, V., MILLER, A. J., RINDI, A. and RAJU, M. R., 1970. Phys. Med. Biol. 15 643.
- SUIT, H. D. 1969. Introduction: Statement of the problems pertaining to the effect of dose fractionation and total treatment time on response of tissue to X-irradiation. In Carmel Conference proceedings: Time and dose relationships in radiation biology as applied to radiotherapy. Brookhaven National Laboratory Report BNL-50203 (C-57), p. vii.
- SULLIVAN, A. H. and BAARLI, J. 1968. Phys. Med. Biol. 13 435.
- TAYLOR, M. C., PHILIPS, G. C. and YOUNG, R. C. 1970. Science 169 377.
- TISLJAR-LENTULIS, G. M., BOND, V. P., ROBERTSON, J. S. and MOORE, W. H. 1971. Radiation Res. 46 16.
- TODD, P. W. 1971. The prognostic value of cellular studies in evaluating new accelerator beams for therapy. Los Alamos Scientific Laboratory Report LA=4653-MS.

TURNER, J. E., DUTRANNOIS, J., WRIGHT, H. J., BAARLI, J., HAMM, R. N. and SULLIVAN, A. H. 1970. Calculation of negative and positive pion depth-dose curves and comparison with experiment. I. Parallel uniform beams. CERN Report DI/HP/32.

VAN PUTTEN, L. M. and KALLMAN, R. F. 1968. J. Natl. Cancer Inst. 40 441.

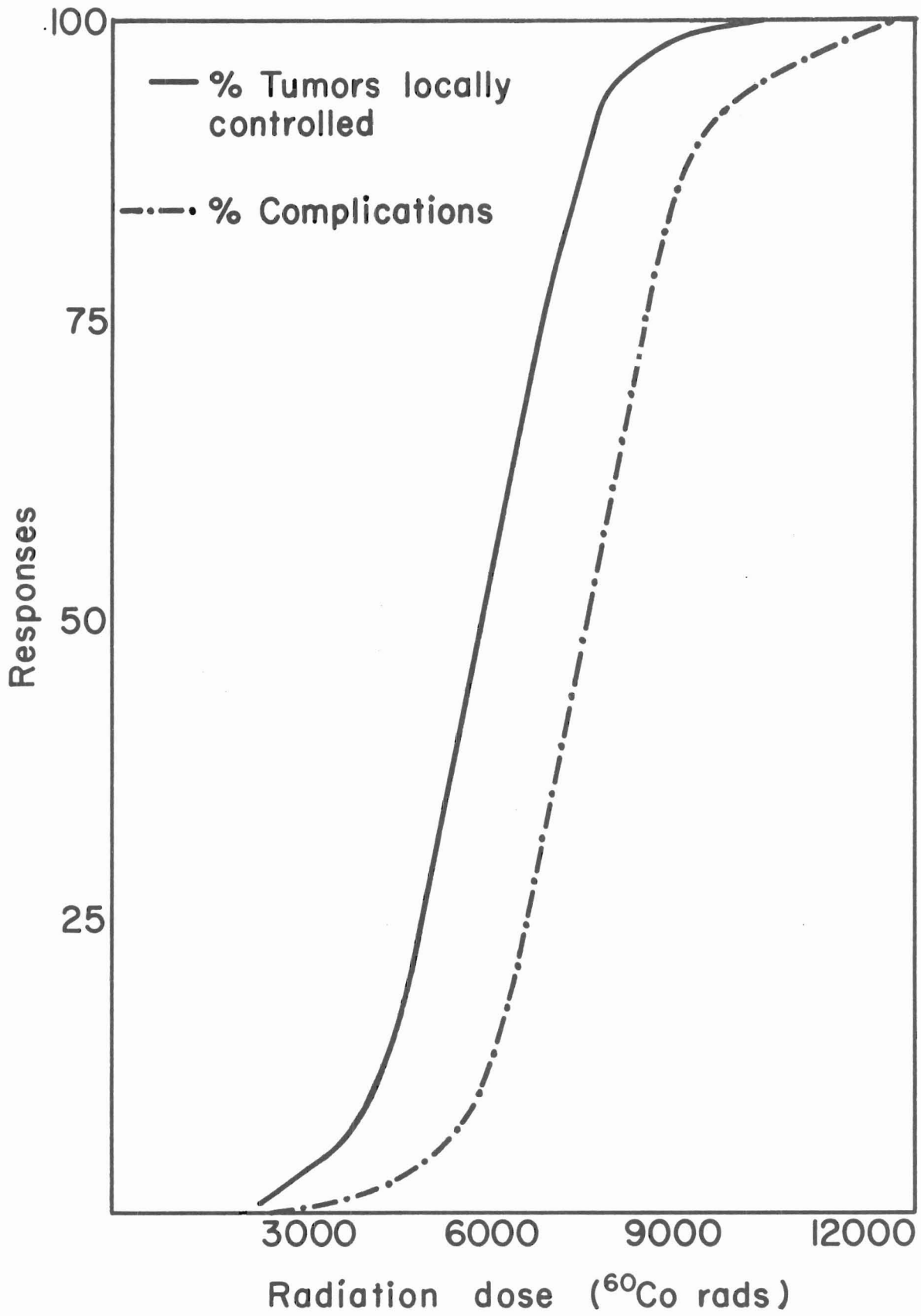
WHITMORE, G. F. 1971. Potential uses of π^- mesons for radiotherapy.

Invited talk, TRIUMF seminar, Vancouver, B. C., May 1971.

FIGURE CAPTIONS

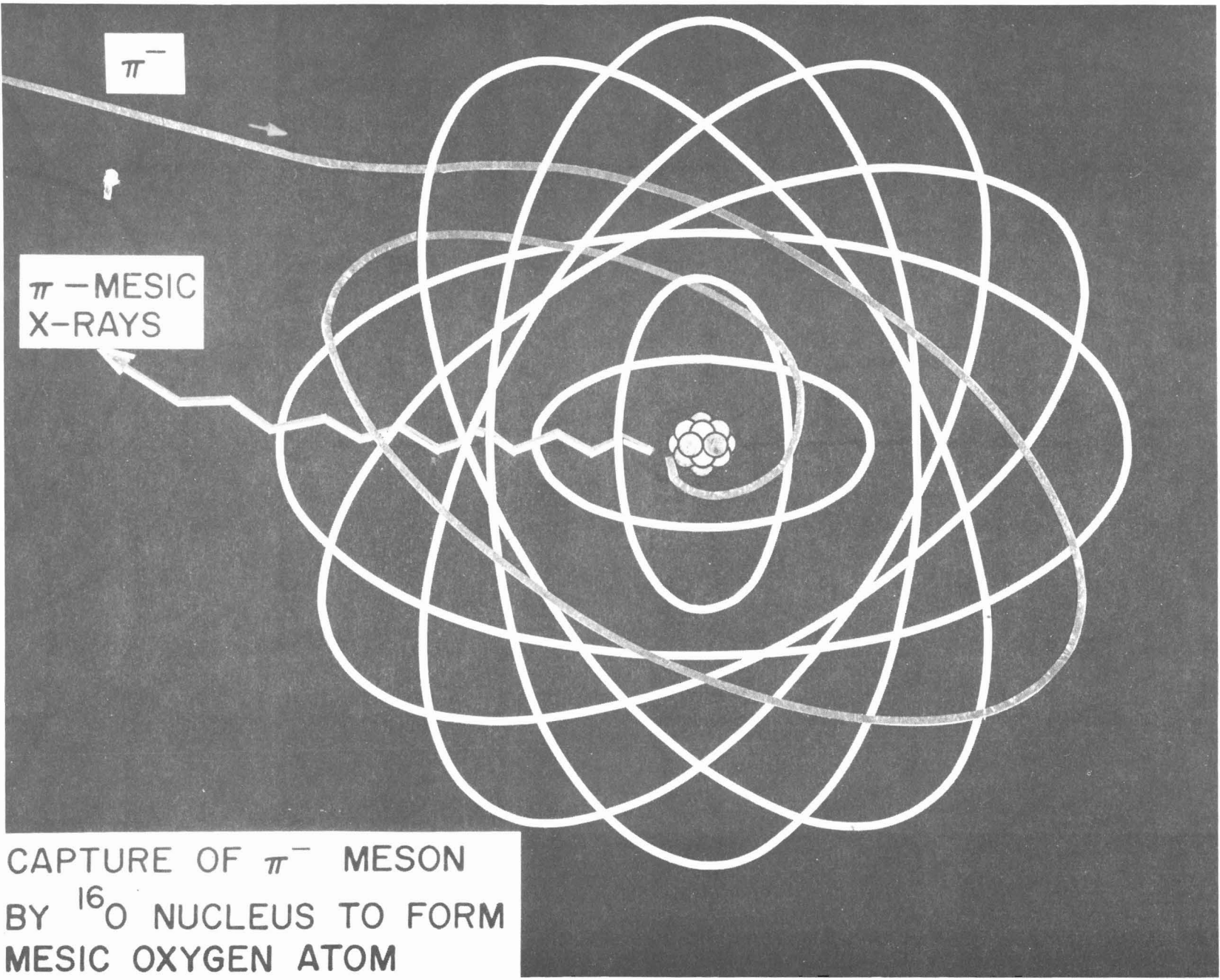
- Fig. 1. General relationship between probability of local tumor control and production of complications as a function of ^{60}Co dose in rads. (Courtesy of Boone and Wiley.)
- Fig. 2. Sketch showing pion capture by atom and the resulting emission of mesic X-rays and pion absorption in the nucleus.
- Fig. 3. Examples of capture of negative pions and the resulting nuclear disintegrations in the light elements carbon, nitrogen, and oxygen as observed in nuclear emulsions. The pion traces are labeled π^- ; the stars produced following their capture have various numbers of prongs. (Courtesy of Powell, Fowler, and Perkins.)
- Fig. 4. Experimental setup for producing a pion beam.
- Fig. 5. Range versus energy for pions in water.
- Fig. 6. Energy versus momentum for pions.
- Fig. 7. Percentage of original π^- flux remaining after a 10-m and 5-m drift.
- Fig. 8. A normalized central-axis depth-dose curve in water for an incident beam of π^- of momentum 190 ± 5 MeV/c with contamination (65% π^- , 25% e^- , 10% μ^-).
- Fig. 9. A normalized central-axis depth-dose curve in water for an incident beam of π^- of momentum 190 ± 5 MeV/c (pure beam).
- Fig. 10. The dE/dx distribution of a contaminated π^- beam at the peak of depth-dose distribution (25.5 cm of water). Calculated for an incident gaussianly distributed momentum distribution 190 ± 5 MeV/c. The contribution of each component is shown. The beam was assumed to be composed initially of 65% π^- , 25% electrons, and 10% muons. (The energy lost by a particle in traveling through a unit distance is called linear energy loss and is usually denoted by dE/dx expressed in $\text{MeV.g.}^{-1}\text{cm}^2$. Sometimes it is also expressed in KeV/μ . In water $10 \text{ MeV.g.}^{-1}\text{cm}^2 = 1 \text{ KeV}/\mu$.)
- Fig. 11. Depth-dose distribution of 65 MeV π^- and π^+ pure beams in water.
- Fig. 12. The 10-day growth plotted as a function of dose at the peak of π^- beam.
- Fig. 13. Survival curves of human kidney cells in culture (T_1) for π^- mesons at the peak of the depth-dose distribution and for ^{60}Co γ -rays.

Fig. 14. Aerial view of LAMPF facility. (a. Laboratory - Office Building; b. Power substation; c. main equipment aisle; d. Operations Building; and e. Experimental area.



XBL714-3312

Fig. 1



CAPTURE OF π^- MESON
BY ^{16}O NUCLEUS TO FORM
MESIC OXYGEN ATOM

Fig. 2

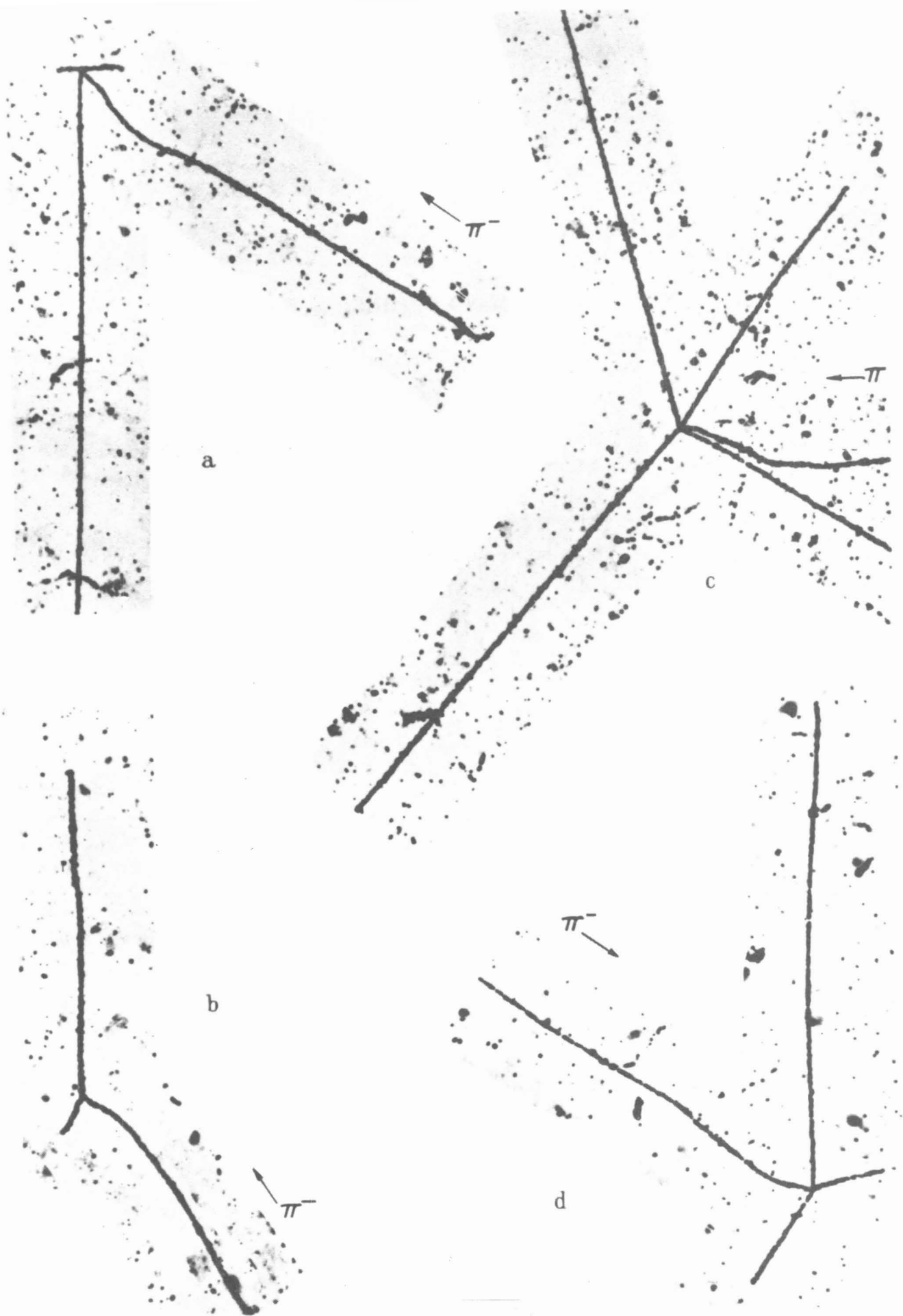
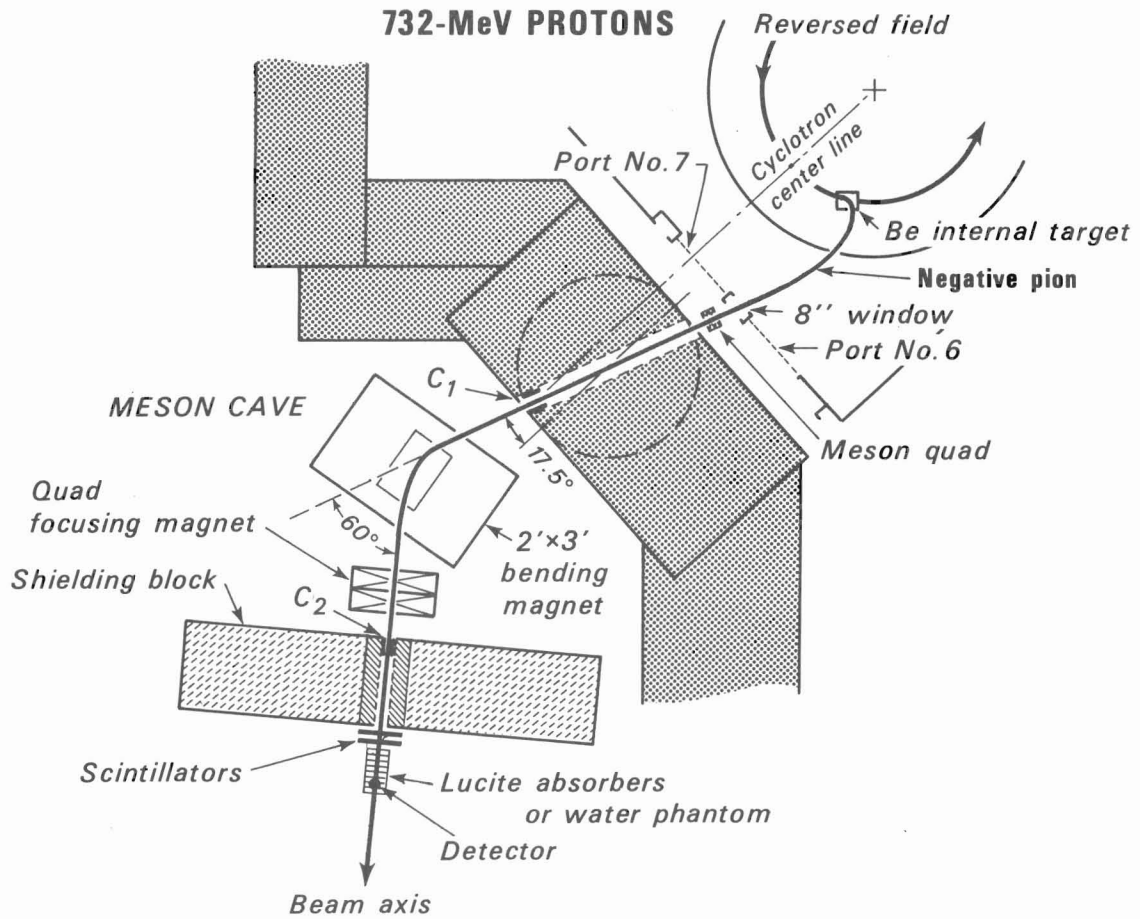
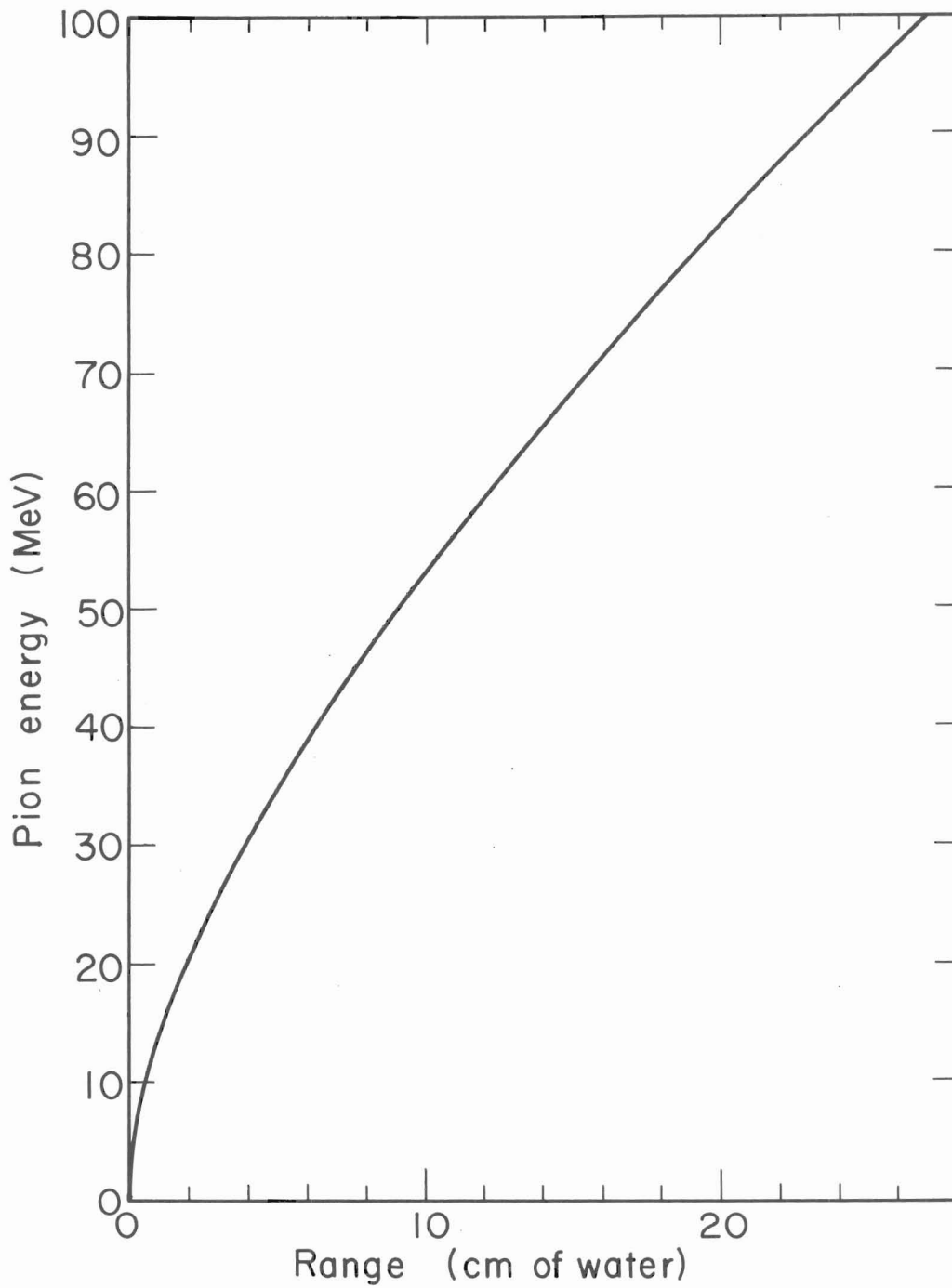


Fig. 3



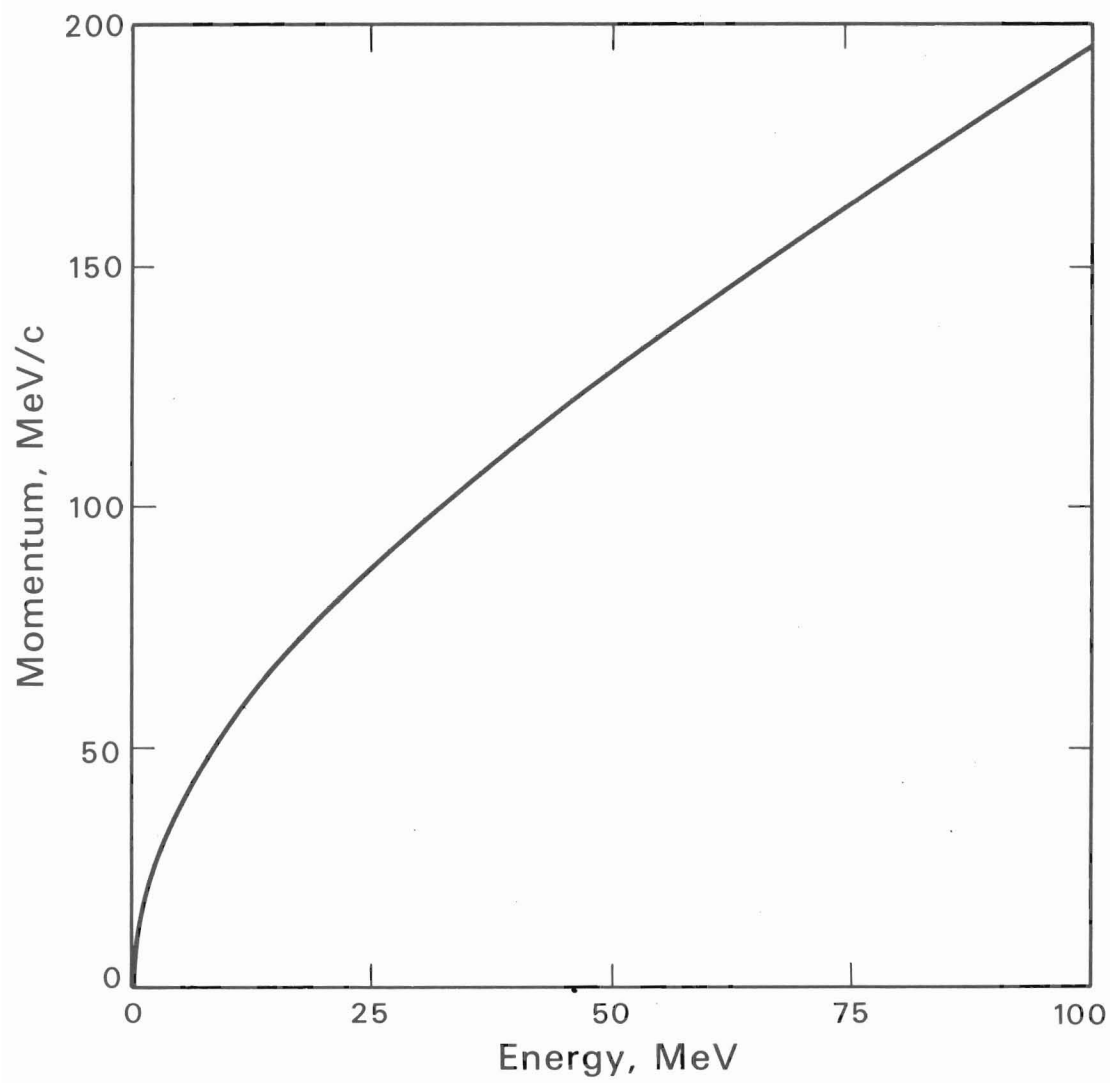
DBL 703 5626

Fig. 4



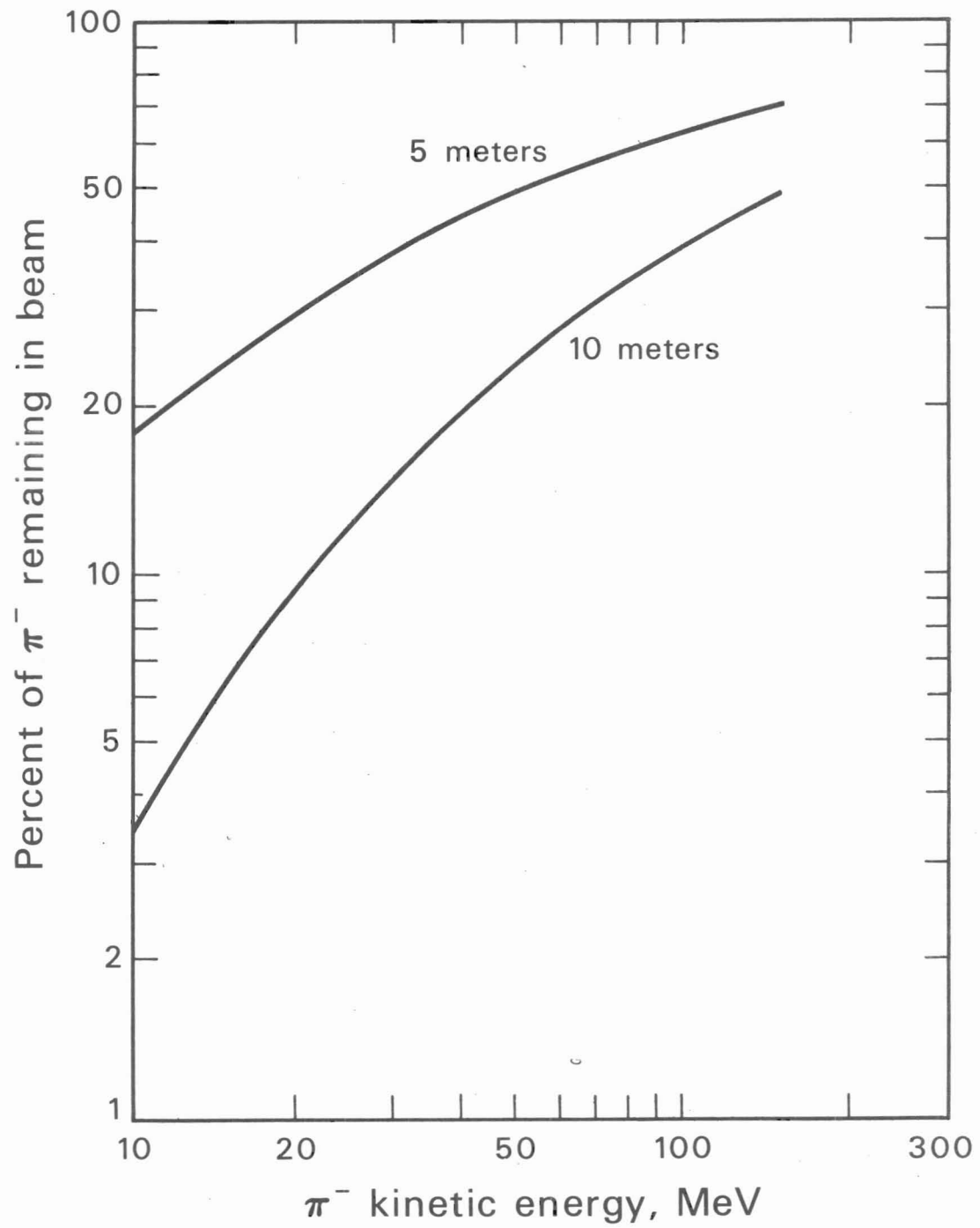
XBL699-3802

Fig. 5



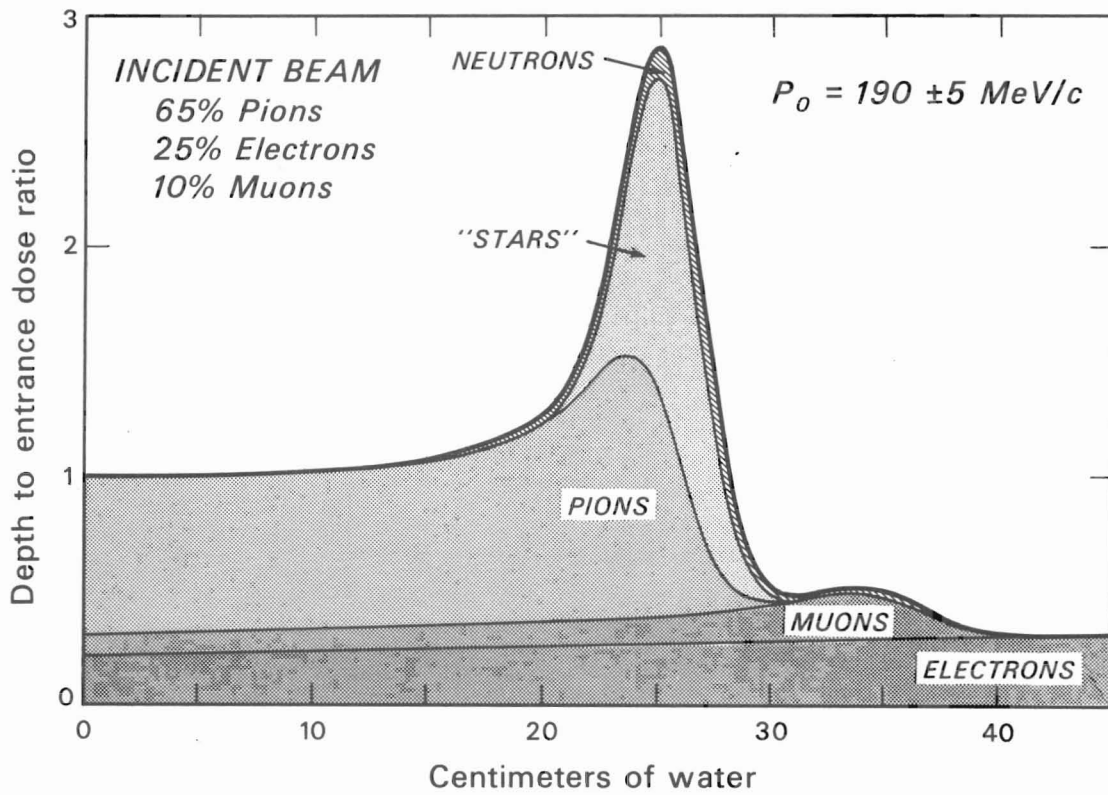
DBL 718-5937

Fig. 6



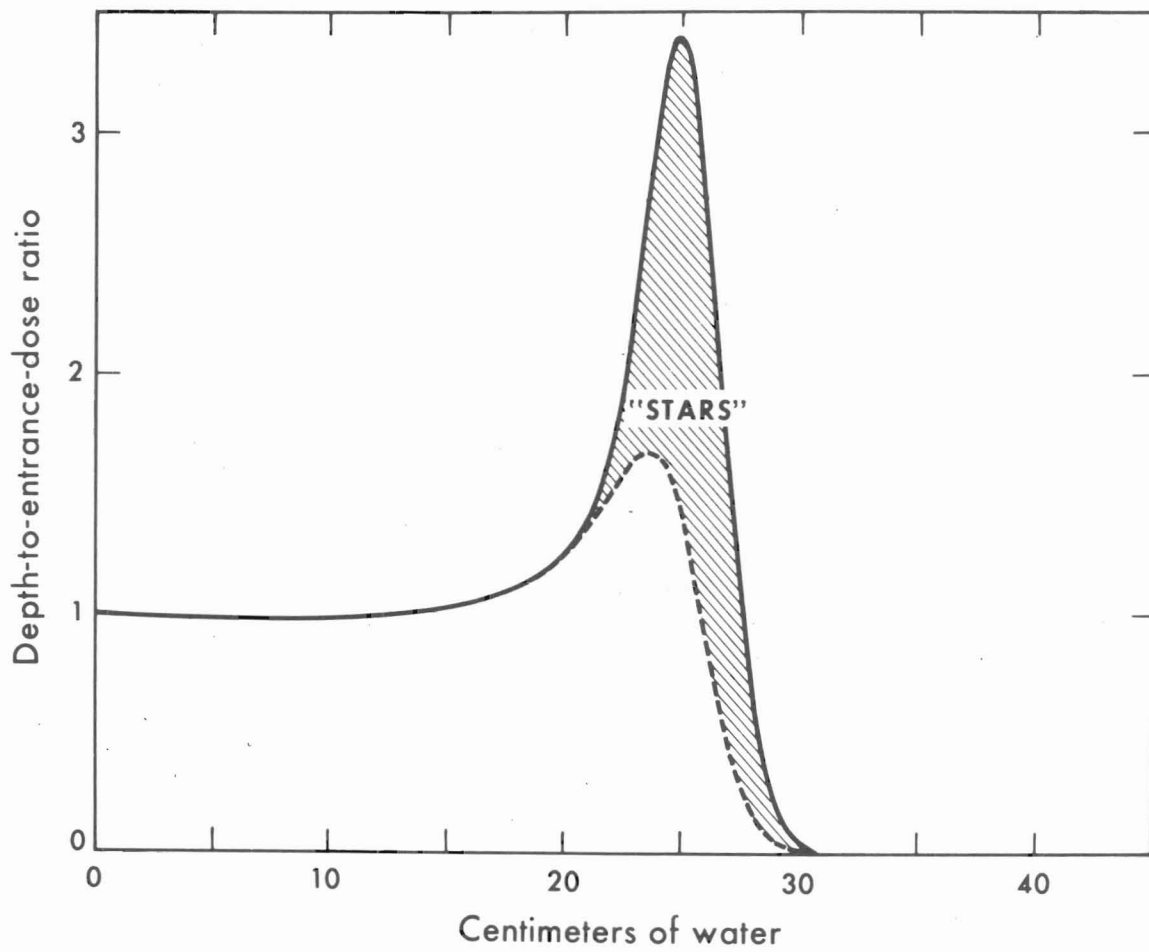
DBL 718-5933

Fig. 7



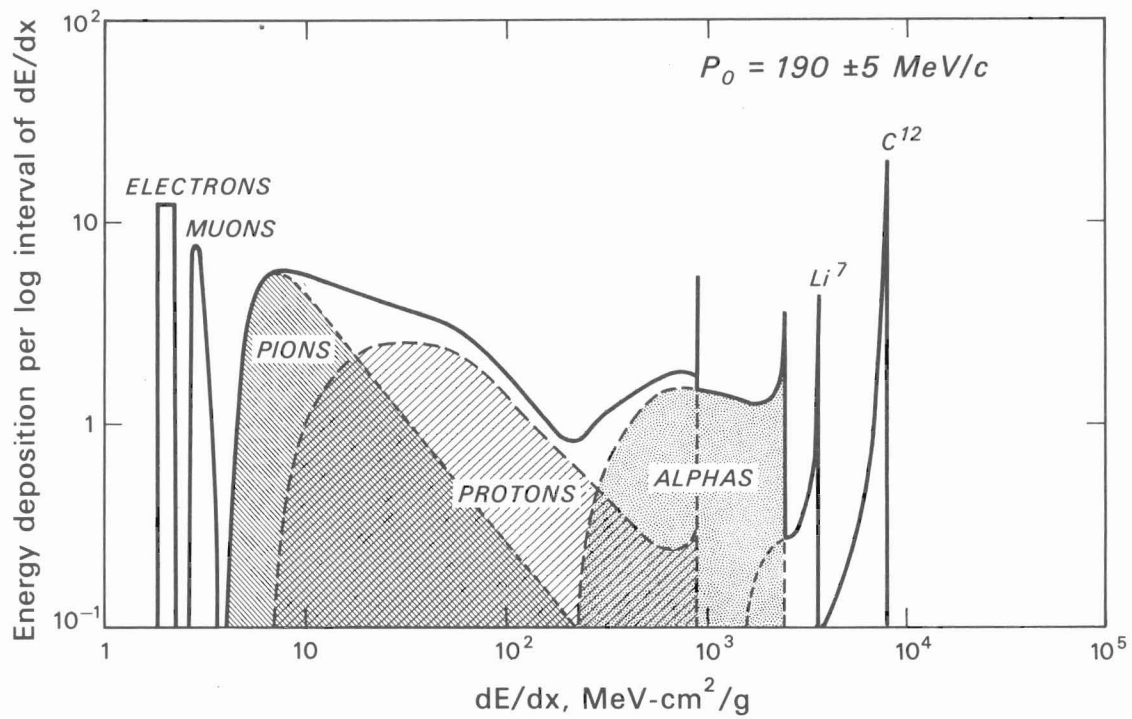
DBL 673-1580

Fig. 8



XBL 673-1229A

Fig. 9



DBL 673-1581

Fig. 10

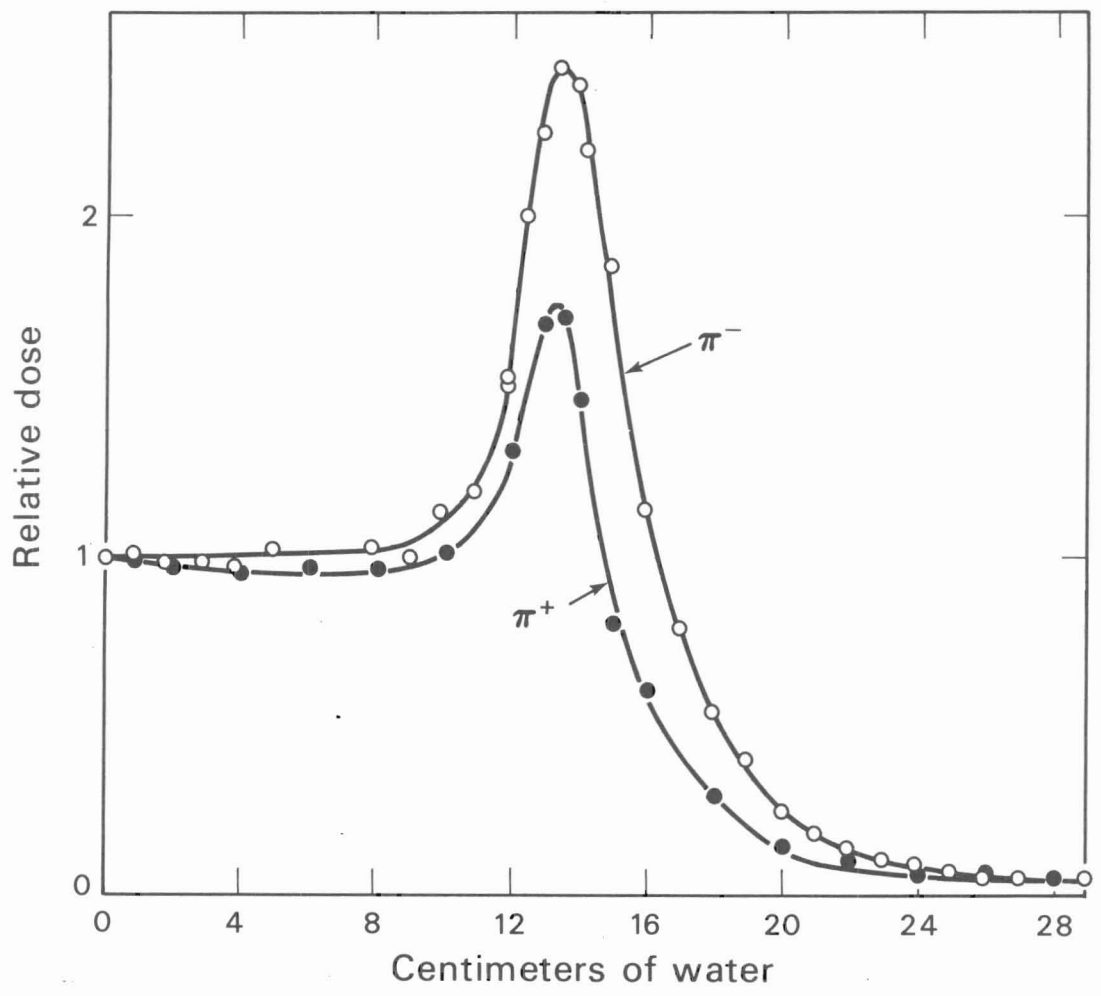
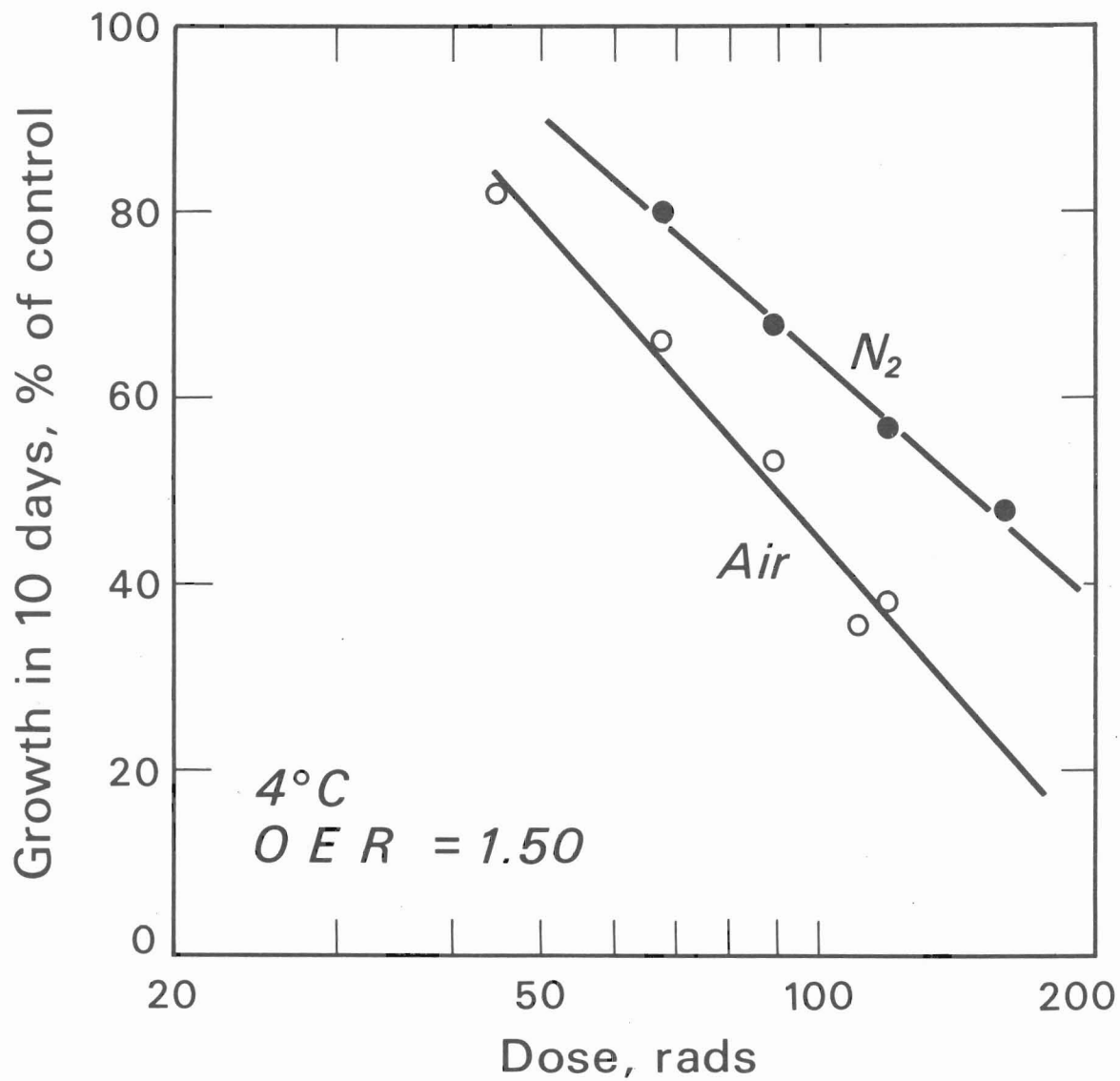
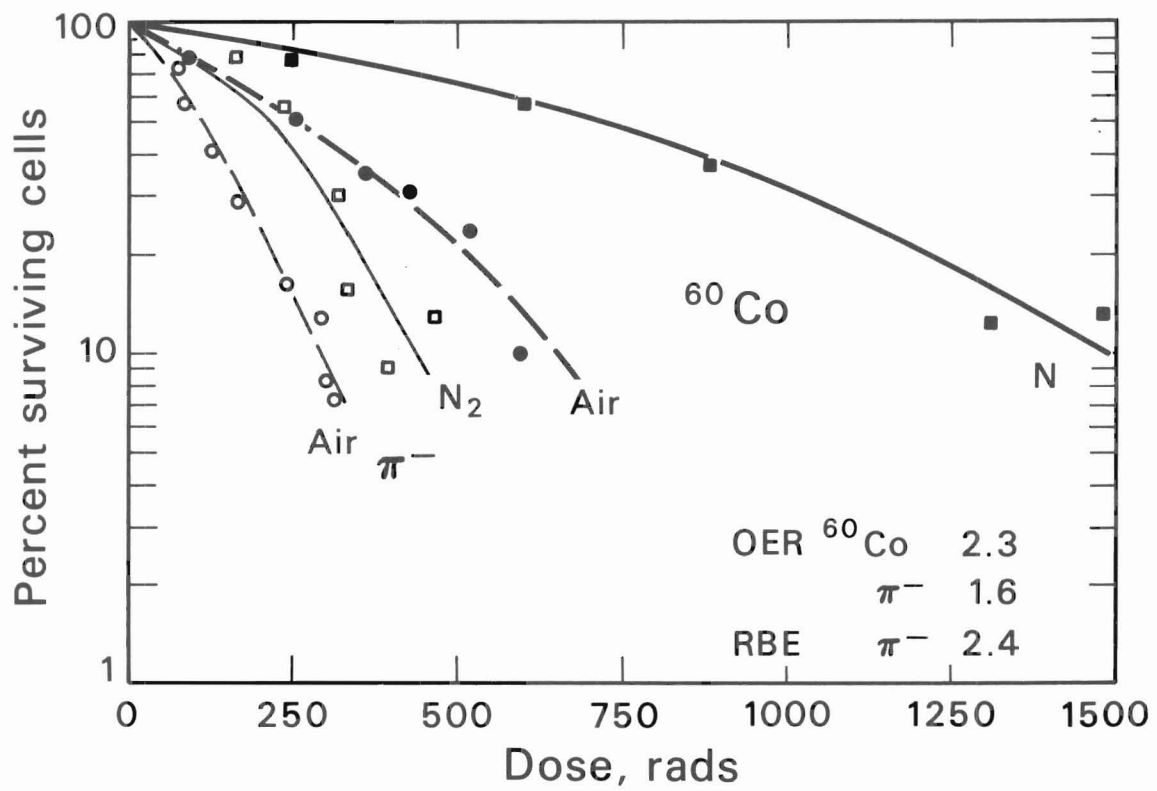


Fig. 11



DBL 6812-5556

Fig. 12



DBL 711-5622

Fig. 13

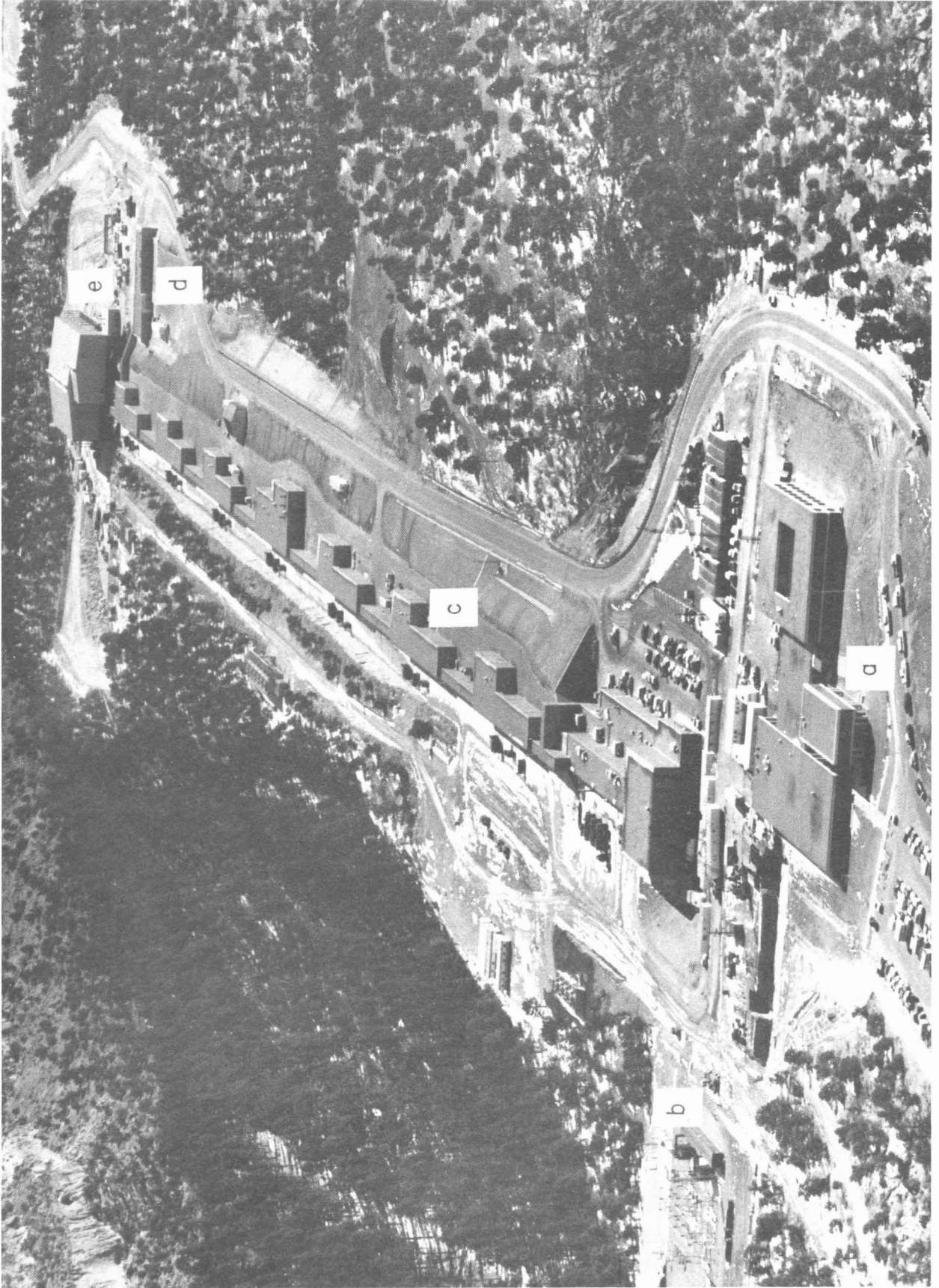


Fig. 14